EPJ Web of Conferences **29**, 00033 (2012)
DOI: 10.1051/epjconf/20122900033

The calculations of thermodynamic and opto-electronics properties of Pb1-xCaxSe semiconducting ternary Alloys

C.Sifi[a1], M. Slimani[1], H. Meradji[2]

[a] Laboratoire LESIMS, Département de Physique, Faculté des Sciences, Université de Annaba, Algeria
[b] Laboratoire de Physique des Rayonnements, Département de Physique, Faculté des Sciences, Université de Annaba, Algeria

Abstract. The ab initio full potential linearized augmented plane wave (FP-LAPW) method within density functional theory was applied to study the effect of composition on the structural and electronic properties Pbl-xCaxSe temary alloys. The effect of composition on lattice parameter, bulk modulus, band gap was investigate. Deviations of the lattice constant from Vegard's law and the bulk modulus from linear concentration dependence were observed. In addition, the microscopic origins of compositional disorder were explained by using the approach of Zunger and co-workers. The disorder parameter (gap bowing) was found to be strong and was mainly caused by the chemical charge transfer effect. The volume deformation contributions for all alloys were also found to be significant, while the structural relaxation contributions to the gap bowing parameter were relatively smaller. On the other hand, the thermodynamic stability and optical properties are attempted in the calculations. The calculated refractive indices and optical dielectric constants for the parent compounds show better agreement with the known data when the Moss relation is used. Compositional dependence of the optical and electronic properties studied is also investigated.
Keywords. Materials for opto-electronics, optical properties, FP-LAPW, bowing gap, Banb structure, critical temperature

1 Introduction

Lead chalcogenide compounds semiconductors are expected to be the tunable laser diodes which laser at mid-infrared region between 3 and 4 µm. In this study band gap IV-VI compounds are promising for wave-length optoelectronic applications in laser diodes and in light emitting diodes. They are considered to be mainly utilized in advanced measurement systems for detecting hydrocarbon pollutants in the air [1] and in a new fiber communication system over super-long distances; which has not yet been developed [2]. In order to use this laser diode, it is required to operate it close to room temperature. So far, many efforts have been made to fabricate laser diodes [3-6].

The compositional variation in Pbl-xCaxSe alloys induces significant changes in their physical properties such as electronic band structures and lattice parameters. The possible development of heterostructures based on these new material systems needs a detailed investigation of these alloys. Although the structural and electronic properties of Pb1-xCaxSe alloy has been studied

[a] e-mail : sifichahra@yahoo.fr

experimentally [7,8], to the best of our knowledge no theoretical investigations Pbl_xCaxSe alloys have appeared in the literature. Hence, in order to exploit fully this material for new optical devices, the structural and electronic properties of these alloys need to be investigated in more detail. Motivated by the above considerations, we have carried out a study of this alloy of interest using the full potential linearized augmented plane wave (FP-LAPW) method. The alloys studied crystallize in the cubic phase over the whole range of composition x ($0 \leq x \leq 1$). The concentration of band gap crossover has also been considered. In addition, the thermodynamics and optical properties are investigated. The optoelectronic properties of the semiconductors alloys are essential in the design and fabrication of devices, the refractive indices and the optical dielectric constants of the materials have been to be known as a function of composition.

After a brief description of the computation al details in Section 2, we present the theoretical results in Section 3. Conclusions are summarized in Section 4.

2 Computational methods

We employed the FP-LAPW method to solve the Kohn Sham equations as implemented in the wien2k code [9]. The exchange-correlation contribution was described within the generalized gradient approximation (GGA) proposed by Perdew et al. [10] to calculate the total energy, while for the electronic properties, in addition to the GGA correction Engel- Vosko's (EVGGA) formalism [11] was also applied. The core states of Pb, Ca, and Se atoms were treated self-consistently and fully relativistically relaxed in a spherical approximation, while the valence states were treated self-consistently within the semi-relativistic approximation (no spin-orbit effects included). Wave functions, charge density and potential were expanded inside muffin-tin spheres of radius RMT by using spherical harmonies expansions, while in the remaining space of the unit cell a plane wave basis set was chosen. The plane wave cutoff of Kmax = 8.0/RMT (RMT is the smallest muffin-tin radius) was used for the expansion of the wave function in the interstitial region for all three alloys and the six binary compounds CaSe, and PbSe. Values of RMT were assumed to be 1.9, 2.1 and 2.2 a.u. for Ca, Se, and Pb atoms, respectively. The charge density was Fourier expanded up to Gmax = 14 (Ry)1-2. The maximum l value for the wave function expansions inside the spheres was confined to lmax=10. Meshes of 47 k-points for binary compounds and 125 k-points for alloys were used in the irreducible wedge of the Brillouin zone. Both the plane wave cutoff and the number of k-points were varied to ensure total energy convergence.

3 Results and discussion

3.1 Structural properties

In the present work we analyze the structural properties of the binary compounds PbSe, CaSe, and their alloys. A rocksalt structure was assumed. The alloys were modeled at some selected compositions with ordered structures described in terms of periodically repeated supercells with eight atoms per unit cell, for the compositions x = 0.25, x = 0.5, x = 0.75. For the structures considered, the calculated total energies at many different volumes around equilibrium were fitted by the Murna-ghan equation of state [15] in order to obtain the equilibrium lattice constant and the bulk modulus for the binary compounds and their alloys. Our results for the materials of interest are compared with the available experimental and theoretical predictions in Table 1. Considering the general trend that the GGA usually overestimates the lattice parameters, our GGA results for the binary compounds are in reasonable agreement with experimental values and other calculated values. Usually, in the treatment of alloy problems, it is assumed that the atoms are located at ideal lattice sites and the lattice constants of alloys should vary linearly with composition x according to Vegard's law [16], however, violations of Vegard's rule have been reported in semiconductor alloys both experimentally [17] and theoretically [18].

The calculated lattice parameters at different compositions of $Pb_{1\_x}Ca_xSe$ alloys exhibit tendency to Vegard's law with a marginal upward bowing parameter equal to -0.014 Å, .respectively, obtained by fitting the calculated values with a polynomial function. This small deviation is due to the relaxation of Pb-Se and Ca-Se bond lengths in $Pb_{1\_x}Ca_xSe$.

Table 1. Calculated lattice parameter (a) and bulk modulus (B) of $Pb_{1-x}Ca_xSe$ ternary alloys at equilibrium volume

	x	Lattice constants a (Å)			Bulk modulus B (GPa)		
		This work	Experiment	Other calculations	This work	Experiment	Other calculations
$Pb_{1-x}Ca_xSe$	1	5.964	5.910[16]	5.968[17]	47.52	51[16]	48.75 [17]
	0.75	6.034			48.05		
	0.5	6.105			48.59		
	0.25	6.166			49.12		
	0	6.217	6.123[19]	6.124[18]	49.66		

The composition dependence of the bulk modulus $Pb_{1\_x}Ca_xSe$ alloys is compared with the results predicted by linear concentration dependence (LCD). A small deviation from LCD is observed, with downward bowing equal to upward bowing equal to 0.01 GPa for $Pb_{1\_x}Ca_xSe$. This deviation is mainly due to the mismatch of the bulk modulus of binary compounds which is in our case very small. It is clearly seen that the bulk modulus decreases by increasing the atomic number of the chalcogen atom. Hence, we conclude that PbSe and CaSe are compressible compared the other chalcogenide compounds, respectively.

3.2 Electronic properties

The self consistent scalar relativistic indirect band gaps of lead calgonate compounds and their alloys were calculated within the GGA and EVGGA schemes. The results for each compound are given in Table2. The values obtained for the band gap of binary compounds within EVGGA are in better agreement with available experimental results in comparison with the values calculated by GGA. It is well known that the GGA usually underestimates the experimental energy band gap [19-22]. This is mainly due to the fact that the functionals within this approximation have simple forms that are not sufficiently flexible to accurately reproduce both exchange-correlation energy and its charge derivative. Engel and Vosko by considering this underestimation constructed a new functional form of GGA which was able to better reproduce the exchange potential at the expense of less agreement as regards exchange energy when compared to experiment. This approach which is called EVGGA yields a better band splitting and some other properties which mainly depend on the accuracy of exchange-correlation potential. However, in this method, the quantities that depend on an accurate description of exchange energy Ex such as equilibrium volumes and bulk modulus are in poor agreement with experiment.

The band gap E_{gABC} of an alloy such as $A_xB_{1-x}C_x$ is not given by the linear concentration x weighted average of the AC(E_{gAC}) and BC (E_{gBC}) gaps but has a quadratic form:

$E_{gABC} = xE_{gAC} + (1-x)E_{gBC} - bx(1-x)$

Where b is known as the bowing parameter. The need to fine tune the band gap of alloys in various device applications has provoked an interest in computing the optical band gap bowing in terms of the constituents elements AC and BC.

Table 2. Gap energy E_g of $Pb_{1-x}Ca_xSe$ ternary alloys at equilibrium volume

	x	Band gap E_g	
		This work	
		GGA	EVGGA
$Pb_{1-x}Ca_xSe$	1	2.105	2.815
	0.75	1.162	1.598
	0.5	0.739	1.312
	0.25	0.440	1.092
	0	0.423	1.079

In order to better understand the physical origins of the gap bowing in Lead calgonate alloys, we follow the procedure of Bernard and Zunger [18] in which the bowing parameter (b) is decomposed into three physically distinct contributions. By considering the fact that the bowing dependence to the composition is marginal, the authors limited their calculations to x=0.5 (50%-50% alloy). The overall gap bowing coefficient at x = 0.5 measures the change in band gap according to the reaction:

$$AB(aAB)+AC(aAC) \rightarrow AB0.5C0.5(aeq) \quad (1)$$

where aAB and aAc are the equilibrium lattice constants of the binary compounds AB and AC, respectively, and aeq is the alloy equilibrium lattice constant. We now decompose reaction (1) into three steps:

$$AB(aAB)+AC(aAC) \xrightarrow{VD} AB(a)+AC(a), \quad (2)$$

$$AB(a)+AC(a) \xrightarrow{CE} AB0.5C0.5(a), \quad (3)$$

$$AB0.5C0.5(a) \xrightarrow{SR} AB0.5C0.5(aeq) \quad (4)$$

The first step measures the volume deformation (VD) effect on the bowing. The corresponding contribution to the total gap bowing parameter bVD represents the relative response of the band structure of the binary compounds AB and AC to hydrostatic pressure, which here arises from the change of their individual equilibrium lattice constants to the alloy value a=a(x) (from Vegard's rule). The second contribution, the charge-exchange (CE) contribution bCE, reflects a charge transfer effect which is due to the different (averaged) bonding behavior at the lattice constant a. The final step measures changes upon passing from the unrelaxed to the relaxed alloy by bSR. Consequently, the total gap bowing parameter is defined as:

$$b = bVD + bCE + bSR, \quad (5)$$

$$bvD = 2[\varepsilon AB(aAB) - \varepsilon AB(a) + \varepsilon Ac(aAc) - \varepsilon Ac(a)], \quad (6)$$

$$bCE = 2[\varepsilon AB(a) + \varepsilon AC(a) - 2\varepsilon ABC(a)], \quad (7)$$

$$bSR = 4[\varepsilon ABC(a) - \varepsilon ABC(aeq)], \quad (8)$$

where ε is the energy gap that has been calculated for the indicated atomic structures and lattice constants. All terms in Eqs. (6)-(8) are calculated separately via self-consistent band structure calculations within density functional theory and the results are given in Table3. The total gap bowing for all the three alloys were found to be mainly caused by the charge transfer contribution bCE. It is due to the large electro-negativity difference between atoms. Indeed, the significant role of bCE is correlated with the ionicity factor difference among constitute binary compounds PbSe (fi=0.086) and CaSe (fi=0.380). These values are calculated using the Pauling's scale[27]. The volume –deformation term bVD contributes to the bowing parameter at smaller magnitude. The weak contributions of bVD can be correlated to the small mismatch of the lattice constants of the corresponding binary compounds. The contribution of the structural relaxation bSR is small in the three alloys. Finally, it is clearly seen that our EVGGA values for bowing parameters are larger than the corresponding values within GGA.

Table 3. Decomposition of the optical bowing into volume deformation (VD), charge exchange (CE), and structural relaxation (SR) contributions compared with that obtained by a quadratic fit (all values are in eV)

		This work				
		FP-LAPW	Relation 21	Relation 22	Relation 23	Experiment
$Pb_{1-x}Ca_xSe$	0	3.22	3.997	3.695	3.822	4.70 [37]
	0.25	3.81	3.957	3.680	3.811	
	0.5	3.21	3.476	3.434	3.625	
	0.75	2.80	3.105	3.144	3.364	
	1	2.35	2.676	2.665	2.779	2.09 [38]

Alternatively, we calculated the total bowing parameter by fitting the non-linear variation of the calculated band gaps versus concentration with quadratic functions. The results are shown in Fig. 1 and obey the following variations:

Pb1-xCaxS $e \Longrightarrow \begin{cases} E_g^{GGA} = 0.439 - 0.624x + 2.258x^2 \\ E_g^{EVGGA} = 1.137 - 1.236x + 2.826x^2 \end{cases}$ (09)

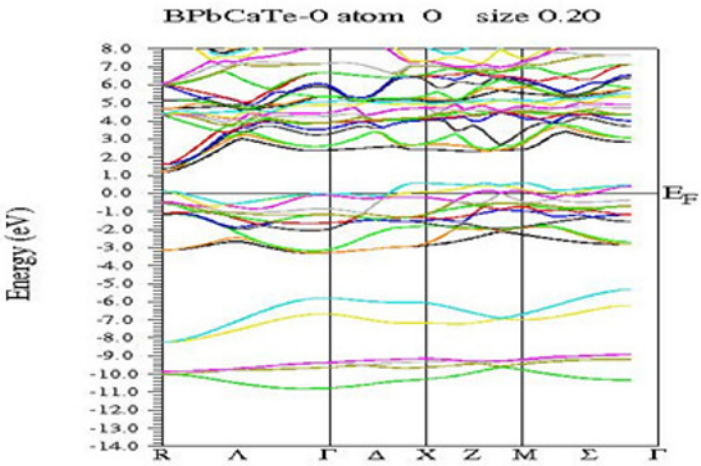

Fig. 1.Composition dependence of calculated band gap using GGA (solid squares) and EVGGA (solid circles) for $Pb_{1-x}Ca_xSe$ alloys

We note that the calculated quadratic parameters (gap bowing) within GGA and EVGGA are close to their corresponding results obtained by Zunger approach.

3.3 Band structures

We describe the electronic properties of Pb1-xCaxSe and for the different concentrations of chalcogenides (x =0.25, 0.50 and 0.75). One preferred to represent only the band structure along high symmetry direction at x = 0.25, since they are similar with only a few changes around the Fermi level (Fig. 3). The band structure is calculated using the calcu- lated lattice constants (as obtained in Section 1. We can observed three main regions in the band structure (Fig. 3): one below −5 eV due to chalcogen s electrons around −10 eV and lead s elec-trons at −7 eV, another one between −5 eV

and Fermi level mainly due to p-chalcogen electrons with a some contribution from p-Pb electrons, and the last one region, just above the Fermi level the biggest contribution from p-Pb electrons. As seen in Fig. 3 the band gap is small and direct. In all cases, the change is observed in the values of the band gap. For better visualizing the behavior of the band gap with the concentration of the chalcogenides, we traced the variation of gap according to the concentration for the semiconductor (Fig1). These alloys present the same behavior, one notes that the values of the gap decrease until the concentration (x = 0.25), starting from this value which the gap starts to increase with the increase in x. Our results of band gap for the binary compounds are in close agreement with others experi-ment [9,28] and theoretical [8–29,30] data (see Table 2), but in the case of alloys there is no theoretical and experiment value to compare with.

3.4 Thermodynamic properties

Focusing on the thermodynamic properties of Pbl_xCaxSe alloys, we calculated the phase diagram based on the regular-solution model [31-33]. The Gibbs free energy of mixing, ΔGm for alloys is expressed as:

$$\Delta Gm = \Delta Hm - T\Delta Sm \quad (10)$$

Where

$$\Delta H = \Omega x(x\text{-}1), \quad (11)$$

$$\Delta Sm = -R[x\ln x + (1-x)\ln(1-x)]. \quad (12)$$

ΔHm and ΔSm are the enthalpy and the entropy of mixing, respectively; Ω is the interaction parameter, R is the gas constant and T is the absolute temperature. Only the interaction parameter Ω depends on the material.

The mixing enthalpy of alloys can be obtained from the calculated total energies as $\Delta Hm=E_{ABxC1-x}\text{-}xE_{AB}\text{-}(1\text{-}x)E_{Ac}$, where $E_{ABxC1-x}$, E_{AB}, and E_{AC} are the respective energies of $E_{ABxC1-x}$ alloy, and the binary compounds AB and AC. We then calculated ΔHm to obtain Ω as a function of concentration. Fig. 4 shows Ω versus x in this manner for $Pb_{l\_x}Ca_xSe$ P alloys. Ω increases almost linearly with increasing x. From a linear fit we obtained

$$Pb_{l\_x}Ca_xSe \implies \Omega\ (\text{Kcal/mol}) = 0.568x + 1.022 \quad (13)$$

The average values of the x-dependent Q in the range $0 \leq x \leq 1$ obtained from these equations for $Pb_{l\_x}Ca_xSe$ alloys is 1.306 Kcal/mol.

Now, we first calculate ΔGm by using Eqs. (10)-(13). Then we use the Gibbs free energy at different concentrations to calculate the T-x phase diagram which shows the stable, metastable, and unstable mixing regions of the alloy. At a temperature lower than the critical temperature Tc the two binodal points are determined as those points at which the common tangent line touches the ΔGm curves. The two spinodal points are determined as those points at which the second derivative o f ΔGm is zero $\delta^2(\Delta Gm)/\delta x^2=0$.

Fig. 2 shows the calculated phase diagrams including the spinodal and binodal curves of the alloys of interest. We observed a critical temperature T_c of 328.39 K for $Pb_{l\_x}Ca_xSe$ alloys. The spinodal curve in the phase diagram marks the equilibrium solubility limit, i.e., the miscibility gap. For temperatures and compositions above this curve a homogeneous alloy is predict. The wide range between spinodal and binodal curves indicates that the alloy may exist as metastable phase. Finally, our results indicate that the calgonate alloys are stable at low temperatures and show a broad miscibility gap surrounded by the binodal line.

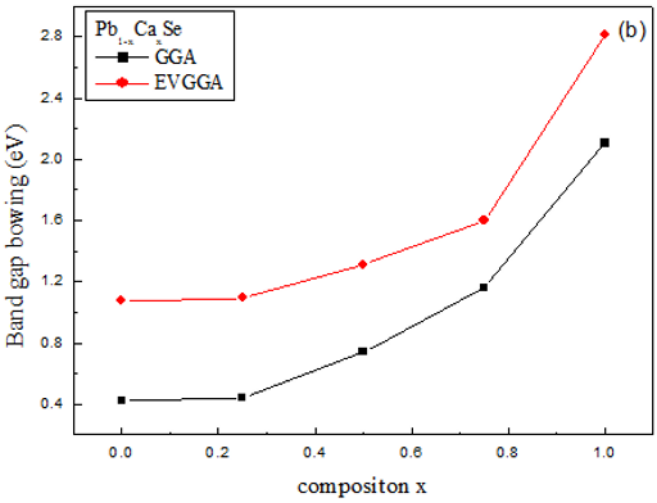

Fig. 2. Band structure of $Pb_{1-x}Ca_xSe$ Te alloys along high symmetry directions in the Brillouin Zone. The Fermi energy is at zero

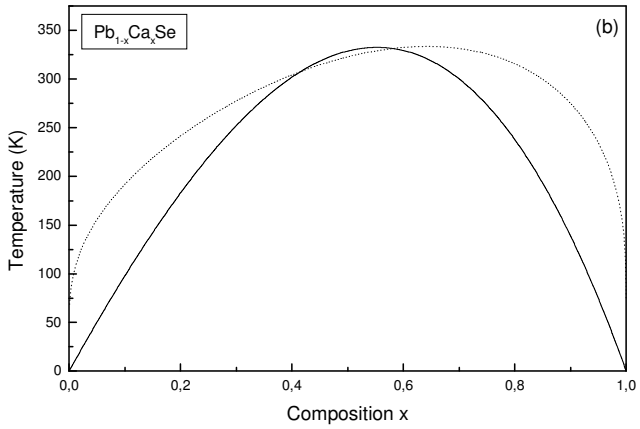

Fig. 3. T-x phase diagram of $Pb_{1-x}Ca_xSe$ Te alloys. Dashed line: binodal curve; solid line: spinodal curve

3.5 Optical properties

The optical properties of matter can be described by the complex dielectric function $\varepsilon(\omega)$, which represents the linear response of a system due to an external electromagnetic field with a small wave vector. It can be expressed as:

$$\varepsilon(\omega)=\varepsilon_1(\omega)+i\varepsilon_2(\omega) \quad (14)$$

Where the ε_1 and ε_2 are the real and imaginary components of the dielectric function, respectively. The imaginary part of the dielectric function in the long wavelength limit has been obtained directly from the electronic structure calculation, using the joint density of states and the optical matrix elements. The real part of the dielectric function can be derived from the imaginary part by the Kramers-Kronig relationship. The knowledge of both the real and the imaginary parts of

the dielectric function allows the calculation of important optical functions. The refractive index n (ω) is given by

$$n(\omega) = \sqrt{\frac{\sqrt{\varepsilon_1^2(\omega)+\varepsilon_2^2(\omega)}+\varepsilon_1(\omega)}{2}} \tag{15}$$

At low frequency (ω=0), we get the following relation:

$$n(0) = \varepsilon^{1/2}(0) \tag{16}$$

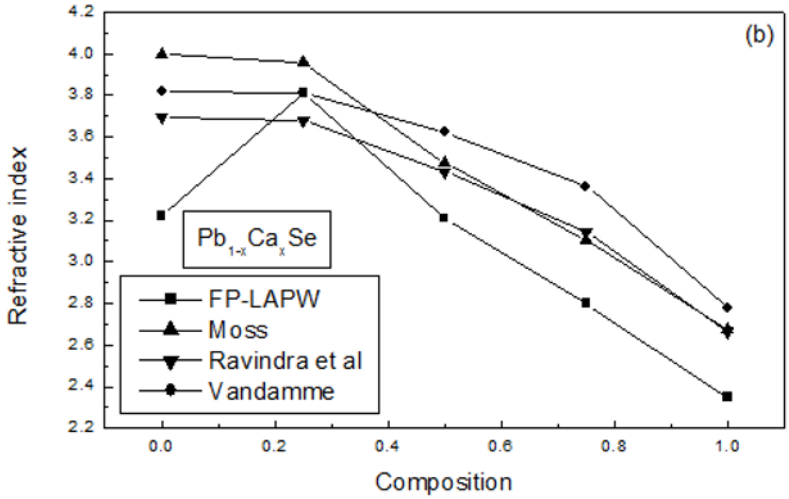

Fig 4. Refractive index for $Pb_{1-x}Ca_xSe$ alloys for different composition x

The refractive index and optical dielectric constants are very important to determine the optical and electric properties of the crystal. Advanced applications of these alloys can significantly benefit from accurate index data. The use of fast non-destructive optical techniques for epitaxial layer characterization (determination of thickness or alloy composition) is limited by the accuracy with which refractive indices can be related to alloy composition. These applications require an analytical expression or known accuracy to relate the wavelength dependence of refractive index to alloy composition, as determined from simple techniques as photoluminescence. A few empirical relations [34-36] relate the refractive index to the energy band gap for a large set of semiconductors. However, in these relations the refractive index n is independent of the temperature and the incident-photon energy. The following models are used:

i) The Moss formula [37] based on atomic model

$$E_g n^4 = k \tag{17}$$

Where E_g is the energy band gap and k a constant. The value of k is given to be 108 eV by Ravindra and Srivastava [34].

ii) The expression proposed by Ravindra *et al.* [35]

$$n = \alpha + \beta E_g \tag{18}$$

With $\alpha = 4.084$ and $\beta = -0.62\ eV^{-1}$.

iii) Herve and Vandamme's empirical relation [36] is given by

$$n = \sqrt{1+\left(\frac{A}{E_g+B}\right)^2} \tag{19}$$

With A = 13.6 eV and B = 3.4 eV.

Table 4 lists the values of the refractive index for the alloys under investigation for some compositions, x, obtained from FP-LAPW calculations and the different models. Comparison with the experimental data has been made where possible. One can note that the values obtained for the refractive index of binary compounds within FP-LAPW method are in better agreement with available experimental results in comparison with the values calculated by the empirical relations.

Table 4. Refractive indices of $Pb_{1-x}Ca_xSe$ for different compositions x

		This work (Zunger)		Quadratic equation	
		GGA	EVGGA	GGA	EVGGA
$Pb_{1-x}Ca_xSe$	b_{VD}	0.141	0.194		
	b_{CE}	2.046	2.427		
	b_{SR}	-0.089	-0.082		
	b	2.098	2.539	2.256	2.827

Using the expressions (14)-(19), the variation of the refractive index for the three alloys of interest as a function of the Ca concentration x has been studied. Our results are plotted in fig.3.

References

1. K. Masumoto, N. Koguchi, S.Takahashi, T. Kiyosawa and I. Nakatani, Sci. Rept. National Res. Inst. Metals **6**, 101 (1985).
2. S. Shibata, M. Horiguchi, K. Jinguji, S. Mitachi, T. Kanamori and T. Manabe. Electron Lett. **17**, 775 (1981).
3. N. Koguchi, T. Kiyosawa and S. Takahashi, J. Crystal Growth **81**, 400 (1987).
4. A.Ishida, K. Muramatsu, H.Takashiba and H. Eujiyasu, Appl. Phys. Lett. **55**, 430 (1989).
5. N. Koguchi and S. Takahashi, Appl. Phys. Lett. **58**, 799 (1991).
6. Mochizuki. H. Iwata. M. Isshiki and K. Masumoto, J. Crystal Growth **115**, 687 (1991).
7. C. Jain, J. R. Willis, and R. Bullogh. Adv. Phys. **39**, 127 (1990).
8. E. A. albanesi, E.L Peltzer, Y. Blanca and A.G. Petukhov, Computational Materials Science, **32**, 85-95 (2005).
9. M. L. Cohen, J.R. Chelikowsky, electronic structure and optical properties of semi conductors, second ed. Springer Series I Solid State Sciences **75** (1989)
10. V. Hinkel, H. Hoak, C. Mariana, L. Sorba, K. Horn, N.E. Christensen, Phys. Rev. B **40**, 5549 (1989).
11. A. Zunger, S.-H. Wei, L. G. Ferreira, and J. E. Bernard, Phys. Rev. Lett. **65**, 353 (1990).
12. P. Blaha, K. Schwarz, G. K. H. Madsen, D. Kvasnicka, and J. Luitz, WIEN2k, an Augmented Plane Wave Plus Local Orbitals Program for Calculating Crystal Properties (Vienna University of Technology, Vienna, Austria, 2001)
13. J. P. Perdew, S. Burke, and M. Ernzerhof, Phys.Rev.Lett. **77**, 3865 (1996).
14. E. Engel and S. H. Vosko, Phys. Rev. B **47**, 13164 (1993).
15. F. D. Murnaghan, Proc. Natl.Acad. Sci. USA **30**, 5390 (1944).
16. H. Luo, R. G. Greene, K. G. Handechari, T. Li and A. L. Ruoff, *Phys. Rev.* B **50**, 16232 (1994).
17. Z. Charifi, H. Baaziz, F. El Haj Hassan and N. Bouarissa, J. Phys.: Condens. Matter 17, 4083 (2005).
18. Mohamed Lach-had, Dimitrios A. Papaconstantopoulos, Michael J. Mehl, Journal of Physics and Chemistry of Solids **63**, 833 (2002).
19. O. Madelung, M. Schulz, H. Weiss (Eds), Numerical Data and Functional Relationships in science and technology Landolt-Bornstei, New Series, **17**, Springer, Berlin, (1983).

20. A. Zaoui and F. El Haj Hassan, J. Phys: Condens. Matter **13**, 253 (2001).
21. L. Vegard, Z. Phys.**5** 17 (1921)
22. J. Jobst, D. Hommel, U. Lunz, T. Gerhard, and G. Landwehr, Appl. Phys. Lett. **69**, 97 (1996)
23. F. El Haj Hassan, Phys. Stat. Sol. b **242**, 909 (2005).
24. P. Dufek, P. Blaha, and K. Schwarz, Phys. Rev. B **50**, 7279 (1994).
25. G. B. Bachelet and N. E. Christensen, Phy. Rev B **31**, 879 (1995).
26. J. E. Bernard and A. Zunger, Phys. Rev. Lett. **34**, 5992 (1986).
27. L. Pauling, Journal of the American Chemical Society, **54,** 3570 (1932).
28. R. Dalven, in: H. Ehrenreich, F. Seitz, D. Turnbull (Eds.), Solid State Physics, **28**, Academic, New York 179 1973.
29. S.Wei, A. Zunger, Phys. Rev. B **55** 13605 (1997).
30. Z. Nabi, B. Abbar, S. Méc ¸ abih, A. Khalfi, N. Amrane, Comp. Mater. Sci. **18** 127 (2000).
31. R. A. Swalin, Thermodynamics of Solids, Wiley, New York, (1961).
32. L. G. Ferreira, S. H. Wei, J. E. Bernard and A. Zunger, Phys. Rev. B **40**, 3197 (1999).
33. L.K. Teles, J. Furthmuller, L.M.R. Scolfaro, J.R. Leite, and F. Bechstedt, Phys. Rev. B **62** 2475 (2000).
34. V. P. Gupta, N.M. Ravindra, Phys. Stat. Sol. b **10**, 715 (1980).
35. N. M. Ravindra, S. Auluck, and V. K Srivastava, Phys. Stat. Sol. b **93** 155 (1979).
36. J. P. L. Herve, L. K. J. Vandamme, Infrared Phys. Technol. **35**, 609 (1994)
37. A. K Walton and T. S. Moss, Proc. Phys. Soc. **81**, 509 (1963).
38. R. R. Reddy, Y. Nazeer Aharnmed, P. Abdul Azeem, K. Rama Gopal, B. Sasikala Devi and T.V.R. Rao, Defence Science Journal, **53**, 239 (2003).